SiF 2026 – The 14th International Conference on Structures in Fire
Queen's University/ York University, Canada, 18 – 21 May 2026

NUMERICAL POST-FIRE DAMAGE QUANTIFICATION OF CONCRETE TUNNELS

Thomas Thienpont[1], Balša Jovanović [2], Ruben Van Coile [3]

ABSTRACT

Tunnel fire resistance is traditionally ensured by imposing temperature limits on the reinforcement and the exposed concrete. Meeting these limits is generally interpreted as proof that the required fire rating is achieved and that the structure remains repairable after a fire. Such temperature-based checks avoid explicit structural analysis and do not provide information on the actual structural damage state, nor the repairability. To move beyond this prescriptive approach, this paper presents a dedicated post-processing tool for SAFIR that quantifies post-fire damage and repairability in reinforced concrete tunnels by combining thermal and mechanically induced damage. The method enables a direct assessment of residual structural performance and supports a more rational evaluation of repairability. The tool is demonstrated through a case study of an existing cut-and-cover tunnel with spalling-sensitive concrete, in which different passive fire protection configurations are analysed. The results show that significant structural damage may develop, even in tunnels equipped with substantial amounts of passive fire protection. Furthermore, the study illustrates how the proposed tool can inform decision-making and contribute to the optimization of passive fire protection strategies for concrete tunnels.

Keywords: Tunnels; performance-based design; post-fire damage; passive fire protection

1 INTRODUCTION

Road tunnels form essential components of modern transport networks, and their uninterrupted availability is of major societal importance. Severe fire events in road tunnels have demonstrated the potential for far-reaching consequences, including fatalities, extensive structural damage, long-term closure, and substantial socio-economic disruption.

Across most international guidelines, life safety is the primary objective, with evacuation and emergency response taking precedence. Although damage limitation is often cited as a secondary goal, structural verification is typically reduced to maximum allowable temperatures of approximately 250 °C for reinforcement and 380 °C for concrete [1][2]. Compliance with these limits is interpreted as proof that the required fire rating is achieved and, implicitly, that the structure will remain repairable after fire exposure.

[1] PhD, Structural Fire Engineer, Pyro Engineering, Ghent, Belgium
e-mail: Thomas.Thienpont@pyro-engineering.com, ORCID: https://orcid.org/0000-0003-1466-3377
[2] PhD, post-doctoral researcher, Ghent University, Ghent, Belgium
e-mail: Balsa.Jovanovic@ugent.be, ORCID: https://orcid.org/0000-0001-5200-5848
[3] Associate professor, Ghent University, Ghent, Belgium
e-mail: Ruben.VanCoile@UGent.be, ORCID: https://orcid.org/0000-0002-9715-6786

These temperature thresholds serve as simplified proxies for structural behaviour rather than direct indicators of structural performance. They do not explicitly capture key mechanisms such as force redistribution caused by restrained thermal expansion, irreversible strength degradation of concrete and steel, or concrete spalling. In practice, verification is frequently carried out under standardised severe fire scenarios, most notably the RWS (Rijkswaterstaat) fire curve, mandated in the Netherlands [2] and the United States (through ASTM E3134-17) [3] and recognised in PIARC guidance [4]. Consequently, reliance on temperature limits alone provides no direct insight into the actual post-fire damage state or the residual loadbearing capacity, and may either overestimate or underestimate the true structural performance under severe fire exposure.

To address these limitations, this paper presents a dedicated post-processing tool for SAFIR [5] that enables a direct quantification of post-fire damage in reinforced concrete tunnels. Rather than relying on temperature limits as a proxy for performance, the tool evaluates both thermal and mechanical damage based on the full thermo-mechanical response obtained from nonlinear finite element analyses. The approach builds the damage quantification methodology for concrete structures proposed by Ni & Gernay [6], and is implemented through Python-based post-processing of SAFIR output. The following section outlines the details of the post-processing tool. The tool is then applied to a case study of an existing cut-and-cover tunnel, considering both a case with and without concrete spalling.

2 METHODOLOGY

2.1 Structural fire modelling in SAFIR

Prior to evaluating the post-fire damage and repairability of a concrete tunnel, a numerical model of the tunnel is to be developed in SAFIR, following the methodology outline in [6]. Herein, a 0.5 m wide slice of the tunnel is analysed as a two-dimensional frame structure. Each change in geometry or reinforcement layout is modelled as a distinct section, resulting in a discretised frame representation of the roof slab and walls (see Figure 2). This approach significantly reduces the computational expense of the model compared to a 3D modelling approach. The 2D simplification of the tunnel geometry neglects longitudinal redistribution effects and therefore does not capture potential three-dimensional load-sharing mechanisms. As such, the 2D model should be interpreted as a conservative representation of the structural response, providing a lower-bound estimate of load-bearing capacity under fire exposure.

The heat transfer analyses are performed on two-dimensional cross-sections of the structural elements. Temperature-dependent material properties for concrete and steel, as well as thermal boundary conditions, are adopted from the Eurocodes [7][8] using the SAFIR SILCON_ETC and STEELEC2 material models, respectively. Standard convective and radiative boundary conditions with emisvity $\varepsilon = 0.7$ and convective heat transfer coefficient of 35 W/m²K are applied at the fire-exposed surface. The unexposed surface is assumed to have very limited influence due to the thickness of the walls and the roof, and is modelled with a convective heat transfer coefficient of 9 W/m²K.

The mechanical response is evaluated using the temperature fields obtained from the thermal analyses of the sections. The 2D frame is subjected to permanent actions including self-weight and soil pressure, combined with a representative variable load on the roof slab. Temperature-dependent constitutive models for concrete and reinforcing steel are adopted in accordance with EN 1992-1-2 [7] using the SAFIR SILCON_ETC and STEELEC2EN material models, respectively. These models also capture the irreversible properties of concrete and steel after fire. The simulation also takes into account the cooling phase to capture irreversible damage, force redistribution, and residual deformations. The analyses are run up to 24 hours to ensure that the structure has cooled down completely. The state of the structure in the last timestep of the analysis is then used as a basis for the post-fire damage assessment presented in the following section.

2.2 Post-fire damage quantification metrics and applicability to concrete tunnels

In this study, post-fire damage is quantified by post-processing the SAFIR output using dedicated Python scripts. For each time step, multiple damage indicators are extracted, allowing the evolution of damage to be evaluated during both the heating and the cooling phase. The metrics are organised in three categories: (i) thermal damage, (ii) mechanical damage at the sectional level, and (iii) mechanical damage at the global structural level. The intent is to translate detailed thermo-mechanical simulation results into damage descriptors that can be interpreted in terms of expected repair scope and functional recovery.

A key point for tunnel applications is that most existing damage classification systems and repair thresholds were developed for building components (e.g. slabs, beams, and columns). Their direct applicability to tunnels is therefore not self-evident, given differences in geometry (very thick cross-sections, sometimes exceeding 1 m in height), restraint conditions (soil–structure interaction and continuity), exposure (severe design fires such as the RWS-fire curve), and performance objectives (availability, durability, and long-term serviceability). In the following, the adopted metrics are summarised and their use for tunnels is discussed, with identified gaps left open for further research and calibration.

2.2.1 Thermal damage

Thermal damage is assessed through the penetration of the 300 °C isotherm (d_{300}) derived from the heat transfer analyses of the sections. Heating to elevated temperatures induces micro- and macro-cracking as well as chemical changes in the cementitious matrix, leading to irreversible losses in stiffness and strength [9]. Experimental evidence indicates that exposure beyond approximately 300 °C can result, after cooling, in a permanent reduction on the order of 30% in compressive strength and 40% in elastic modulus [10]. Concrete that has experienced peak temperatures above 300 °C is commonly assumed to require removal and replacement in repair practice [11]. The d_{300} isotherm divides each cross-section into an outer zone where material properties are considered permanently and severely degraded and an zone with limited thermal damage.

The literature proposes thermal damage states for reinforced concrete members based on ranges of d_{300} isotherm, linked to progressively more invasive repair interventions [6], see Table 1.

Table 1. Fire damage states for the d_{300} isotherm in the sections of the RC members [6]

Damage state	**Penetration depth d_{300} isotherm**	**Repair actions**
DS0	$d_{300} = 0$	No repair required
DS1	$0 < d_{300} < c/10$	Chip, clean and patch damaged region
DS2	$c/10 < d_{300} < c$	Remove damaged concrete in repair area to fully expose rebar; clean by high water pressure; blow off dust/debris with compressed air; place repair material by wet shotcrete process to full depth of repair; cure with sprayed membrane curing compound
DS3	$c < d_{300} < d/4$	Remove concrete in repair area to fully expose reinforcing bars and to the depth of d_{300}; clean by high water pressure; blow off dust/debris with compressed air; place of supplemental rebar; place repair material by wet shotcrete process to full depth of repair; cure with sprayed membrane curing compound
DS4	$d/4 < d_{300}$	Demolish and reconstruct

*c = concrete cover; d = side dimension of the cross-section

In this study, these classifications are adopted as a first estimate to translate the computed d_{300} into repair scope. For tunnel structures, however, the damage classification based on the d_{300} isotherm and the associated repair measures may differ due to the often large dimensions of the structural members. A tunnel-specific calibration of the damage states based on the d_{300} isotherm remains an open point and should be investigated further.

2.2.2 Mechanical damage at the sectional level

The section-level mechanical post-fire damage of the tunnel structure is quantified by identifying concrete cracking and reinforcement yielding, derived from the sectional stress–strain state in SAFIR. These damage indicators capture damage mechanisms that may develop not only in the fire-exposed regions, but also on the cold side of members due to restrained thermal expansion and force redistribution within the structural system.

The damage due to cracking is considered using two bands, linked with the constitutive model for concrete in tension as implemented in SAFIR, see Figure 1. Herein, concrete is considered "lightly cracked" when the tensile strength f_t is exceeded, but where the tensile strain is (softening branch) and still has limited tensile capacity. Severe cracking is defined for parts of the cross-section where the tensile strains exceed the end of the softening branch and have zero residual tensile capacity.

Yielding of the reinforcement is used as an indicator for the formation of plastic hinges. A plastic hinge forms when the tensile reinforcement reaches its yield strength, resulting in a local loss of flexural stiffness and allowing significant rotations to develop without further increase in bending moment. The formation of such a hinge leads to redistribution of internal forces within the structure and is typically accompanied by increased deformations of the affected member.

Unlike for thermal damage, the literature does not currently provide established tunnel-specific damage states based on cracking and reinforcement yielding. Therefore, in this study, a provisional classification is used (see Table 2), but the link to repairability and intervention strategy is not yet investigated.

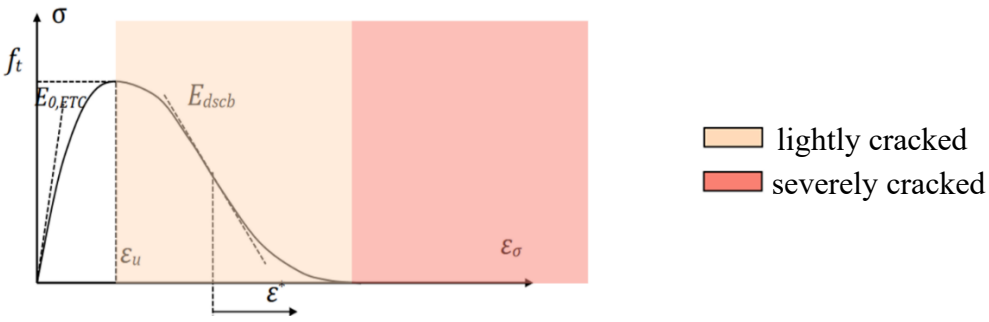

Figure 1. Stress-strain diagram for concrete in tension implemented in SAFIR with indication cracking defitions

Table 2. Fire damage states based on section-level damage

Damage state	**Residual vertical deflection**	**Repair actions**
DS0	No severe cracking, no plastic strains in rebar	No repair required
DS1	Severe cracking, no plastic strains in rebar	Seal cracks
DS2	Severe cracking and plastic strains in rebar	To be studied further

2.2.3 Mechanical damage at the global level

Global mechanical damage is assessed through residual deformations after cooling, extracted from the structural analysis. This metric captures the system-level irreversibility and is affected by restraint effects and force redistributions during the heating and cooling phases of the fire. Residual deformations can continue to increase well into the cooling phase. As such, the SAFIR models should be evaluated for a significant duration after the end of the cooling phase.

To date, no dedicated guidance exists on the damage classification of concrete tunnels based on residual deformations. Therefore, as an initial approach, this study considers the damage classification for concrete buildings, see Table 3. Herein, the residual roof deflection is used as a quantitative indicator of global damage

severity, while acknowledging that acceptable residual deformation limits for tunnels likely also depend on serviceability requirements, waterproofing integrity, and pavement and equipment tolerances. Establishing tunnel-relevant deformation-based damage classes and repair measures is identified as a further research need.

Table 3. Fire damage states based on residual vertical deflection of RC slabs [6]

Damage state	**Residual vertical deflection**	**Repair actions**
DS0	$\Delta_s/l < 1/240$	No repair required
DS1	$1/240 < \Delta_s/l < 1/120$	Clean the surface by high-pressure water; blow off dust/debris with compressed air; place repair material; spray with membrane curing compound
DS2	$1/120 < \Delta_s/l < 1/60$	Demolish and reconstruct slab, beams can be reused
DS3	$1/60 < \Delta_s/l$	Demolish and reconstruct

3 CASE STUDY EXISTING CUT-AND-COVER TUNNEL

The cut-and-cover tunnel examined in this case study consists of two four-lane traffic tubes and a central evacuation shaft, see Figure 2. In the structural analysis, a modified 120-minute RWS fire curve is used, assuming uniform exposure to the walls and ceiling of the affected tunnel tube. The heating phase of the fire is identical to that of the standard RWS curve, but is extended with a dedicated cooling phase, which follows an exponential decay. The latter is based on the experimental observations reported in [12] and a series of numerical analyses of the cooling phase in compartment fires [13].

3.1 Results structural fire model

The results from the heat transfer analyses of two of the sections, and the mechanical analysis of the case study tunnel with a fire in the left tube are depicted in Figure 3 and 4, respectively. When exposed to a 120-minute RWS fire, significant force redistributions occur in the structure, but the structure survives the fire, including the cooling phase. Due to the non-uniform temperature gradients across the walls and the ceiling, restrained thermal expansion results in large changes in the moment line. Notably, at the outer corners and at the connection of the roof slab with the walls of the evacuation tube, the hogging moments increase significantly, see Figure 4 (left). During the cooling phase, the moment redistribution partially reverses; however, at the end of the analysis (24 hours), the bending moments do not return to their pre-fire values, indicating permanent alterations in the internal force distribution of the structure. The graphs in Figure 4 (right) depicting the axial forces show a similar trend. During the heating phase, the compression force at the bottom of the fire-exposed inner wall increases significantly, while the compression force in the inner wall next to the unaffected tube is strongly reduced. During cooling, this trend reverses, although a permanent change in the forces exists compared to the force state before the fire.

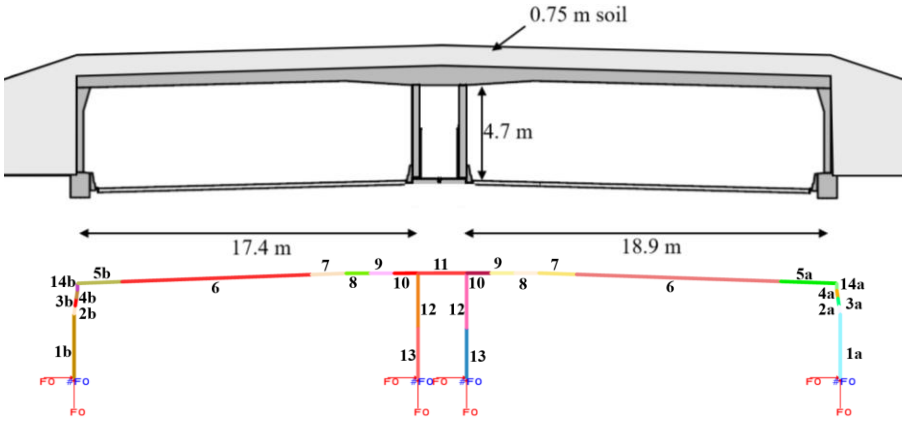

Figure 2. (top) tunnel cross-section; (bottom) representation in SAFIR model, including numbering sections.

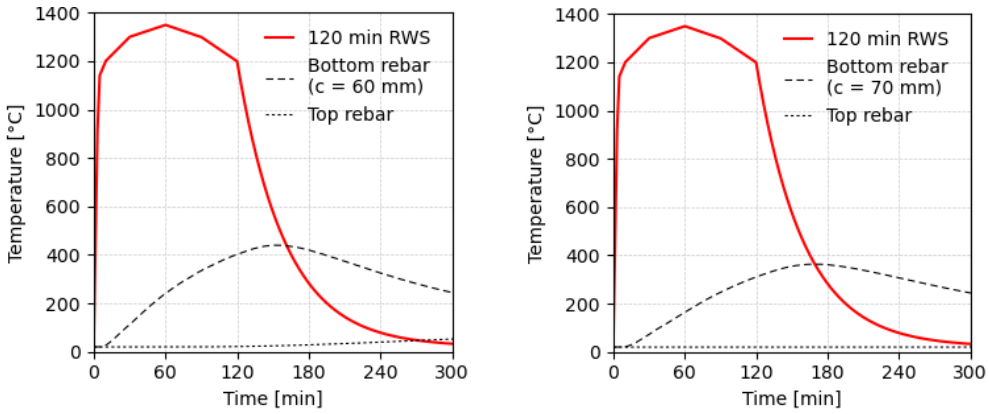

Figure 3. Heat transfer analyses for the outer walls (left) and roof slab (right), considering a 120 RWS fire curve with cooling.

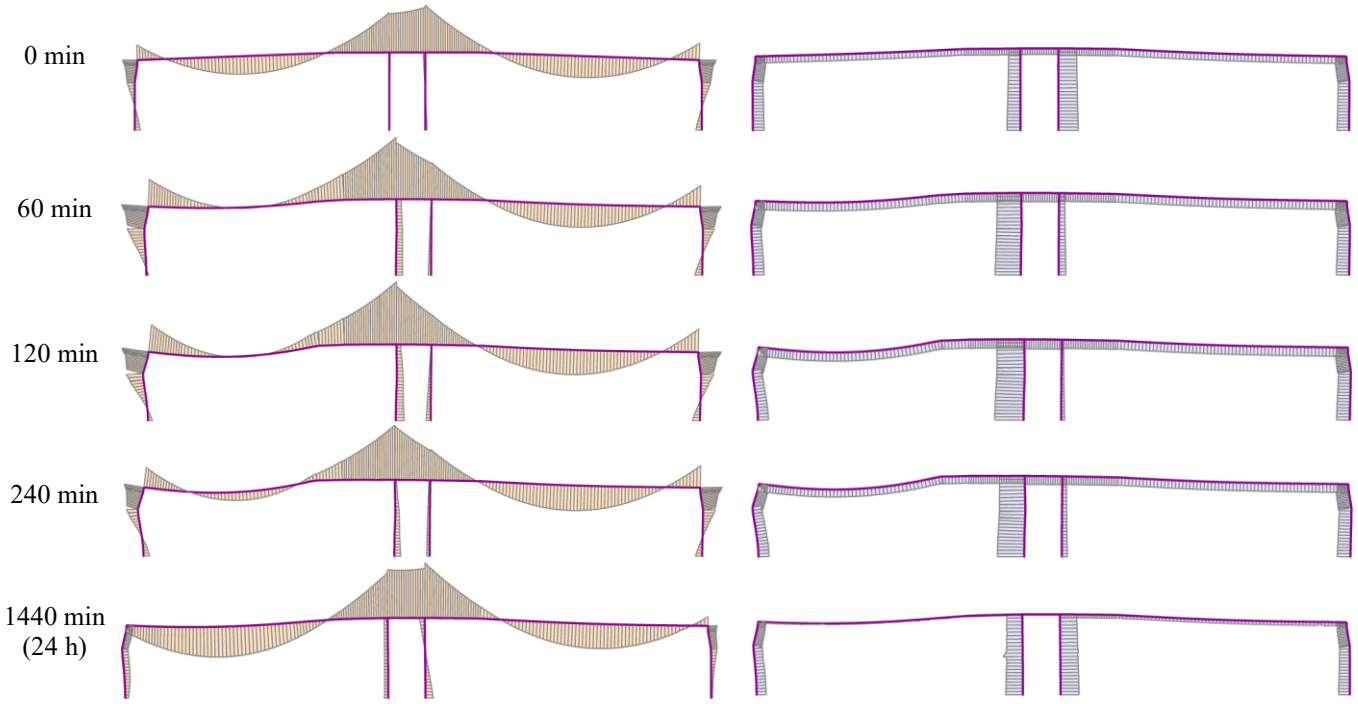

Figure 4. Deformations (5x scaling) and development of bending moments and axial forces, 120-minute RWS fire in the left tube.

3.2 Post-fire damage and repairability

Figure 5 shows the evolution of the damage state in terms of cracking and plastic hinge formation over time for a 120-minute RWS fire in the left tunnel tube. The fire-induced structural damage is shown to increase progressively during the heating phase. The results further demonstrate that the structural damage continues to evolve during the cooling phase. In particular, the total length of severely cracked sections increases significantly after the end of the heating phase at 120 minutes. Neglecting the cooling phase would therefore lead to an underestimation of structural damage in concrete tunnels.

The continued deterioration is further evidenced by the formation of a third plastic hinge in the outer wall of the fire-exposed tube during cooling. This behaviour is attributed to irreversible strength degradation of heated concrete combined with ongoing force redistribution. Damage is also not confined to directly exposed regions. During cooling, limited severe cracking develops at the bottom of the outer wall of the non-exposed tube, illustrating the effects of restraint and global structural interaction. Based on the observed crack pattern and

the three regions where plastic hinges form, the global mechanical damage state of the tunnel after fire is classified as DS2 in accordance with Table 2. However, further research is required to provide robust guidance on the repairability of regions where plastic hinges have developed.

Figure 6 presents the thermal damage classification. Based on the criteria defined in Table 1, the roof and the outer wall of the exposed tube are classified as DS3 and are therefore considered repairable. The upper half of the directly exposed wall of the evacuation tube is classified as DS4 and is consequently deemed unrepairable.

Figure 7 shows the midspan deflection of the roof slab of the left tunnel tube over time. The results illustrate that deformations do not stabilise at the end of the heating phase, but continues to increase during the cooling phase before partially recovering as the structure cools further. Based on the residual deflection of 67.1 mm, the roof slab is classified as damage state DS0 in accordance with Table 3 ($\Delta_s/l = 0.0038 < 1/240$).

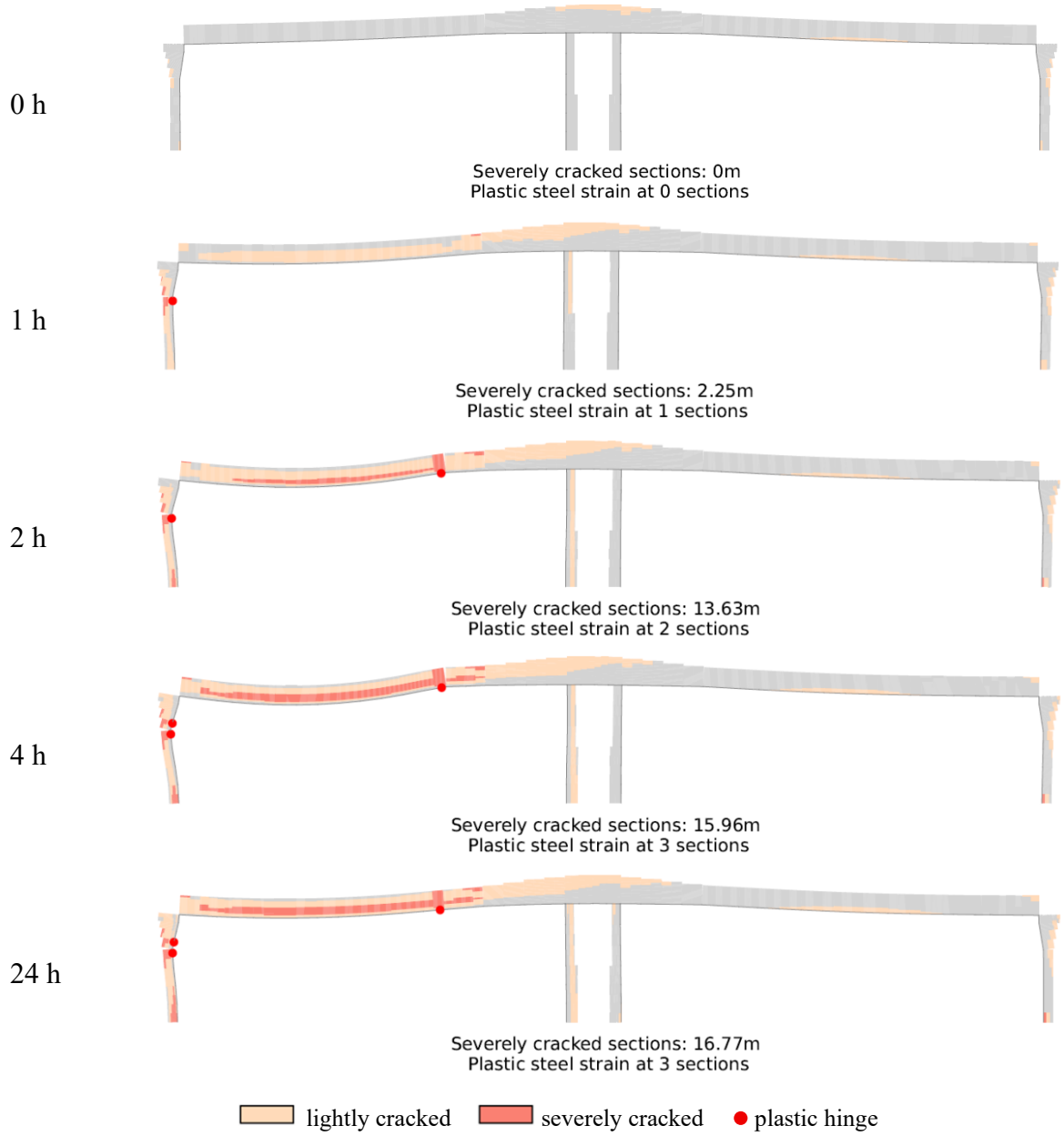

Figure 5. Deformations (5× scaling), cracked regions, and plastic hinge formation over time for a 120-minute RWS fire in the left tunnel tube.

Figure 6. Thermal damage classification after a 120-minute RWS fire in the left tunnel tube.

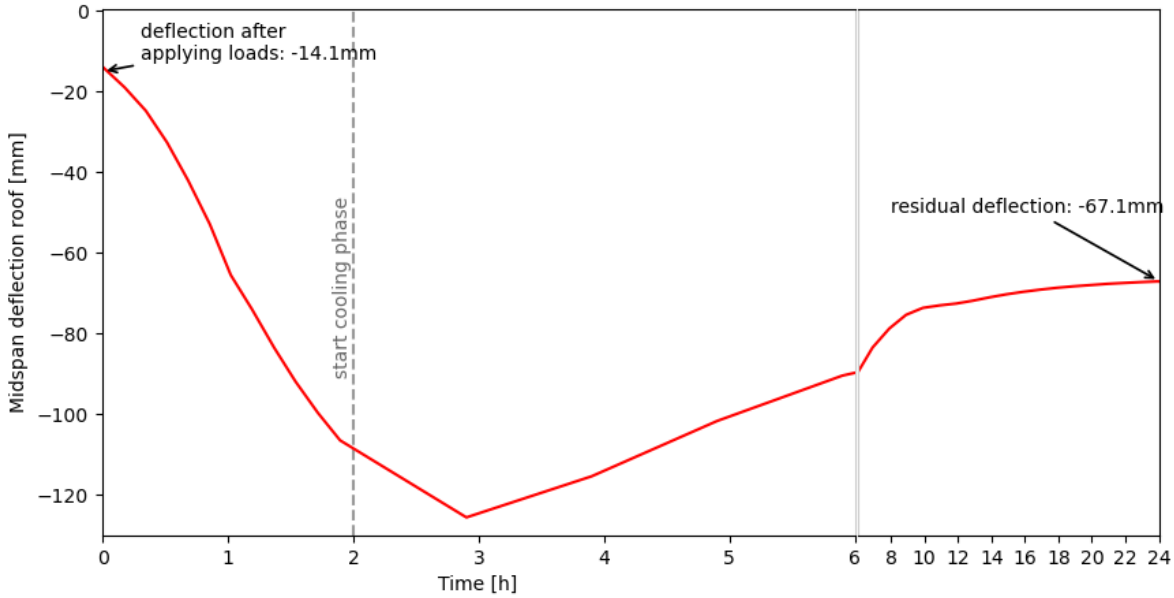

Figure 7. Evolution of the mid-span deflection of the roof slab during and after a 120-minute RWS fire in the left tunnel tube.

Overall, these results demonstrate that the post-fire damage in concrete tunnels cannot be assessed based solely on peak temperatures or heating-phase response. Both mechanical and thermal damage continue to evolve during cooling, influencing the final damage classification. A comprehensive post-fire assessment must therefore integrate cracking, plastic hinge formation, thermal degradation, and residual deformations to obtain a realistic evaluation of structural condition and repairability.

3.3 Influence of passive fire protection

To demonstrate the practical application of the developed damage quantification tool in supporting tunnel asset managers, the post-fire damage of the tunnel is evaluated for four levels of passive fire protection, as shown in Figure 8. In all cases, protected structural members are assumed to be covered with 30 mm thick calcium-silicate boards, significantly reducing their thermal exposure. In the thermal analyses, the boards are modelled with the following material properties: density 870 kg/m³, thermal conductivity 0.175 W/(m·K), and specific heat capacity 750 J/(kg·K). In the mechanical analyses, the mechanical properties of the boards are neglected. Their structural strength is not considered, no force transfer between the boards and the concrete is assumed, and the additional dead load resulting from the boards is disregarded, as it is small compared to the other applied loads. Each scenario considers a 120-minute RWS fire in the left tunnel tube.

Figure 8 presents the resulting mechanical damage patterns. The graphs indicate both the location and extent of concrete cracking, distinguishing between light and severe cracking. Sections where plastic strains develop in the reinforcement are marked, reflecting substantial force redistribution within the structure. The results clearly demonstrate the beneficial effect of targeted passive fire protection. Protecting the roof and upper wall regions substantially reduces post-fire damage. In contrast, extending the protection to the lower half of the

tunnel walls provides only limited additional benefit, as observed by comparing cases 3 and 4. For this tunnel configuration, such additional protection would therefore be structurally marginal and economically unjustified.

Furthermore, the results for case 2 show that while cracking within the protected region is significantly reduced, increased cracking may develop in adjacent unprotected regions. This highlights the importance of considering force redistribution and boundary effects when defining the extent of passive fire protection.

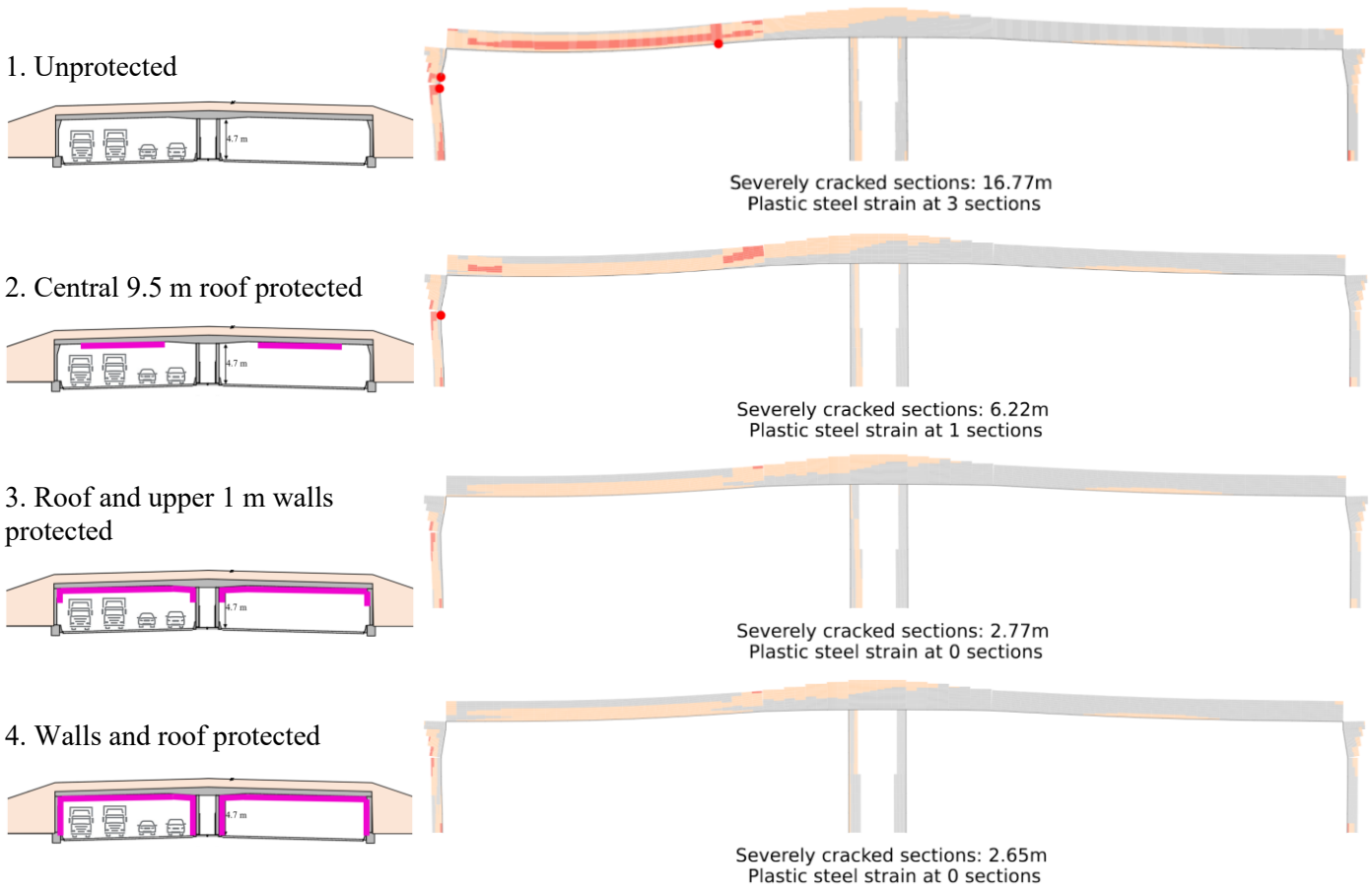

Figure 8. Deformations (5x scaling), cracked areas and plastic hinges over time, considering four levels of protection with 30 mm thick calcium-silicate boards, considering a 120-minute RWS fire in the left tube.

4 CONCLUSIONS

This paper presented a dedicated post-processing tool for SAFIR that enables a direct quantification of post-fire damage and repairability in reinforced concrete tunnels. By combining thermal, sectional mechanical damage, and global damage, the approach moves beyond traditional temperature-limit verification and provides a performance-based assessment of the structural condition after fire.

The application of the tool to an existing cut-and-cover tunnel subjected to a 120-minute RWS fire demonstrated that significant force redistribution, cracking, and plastic hinge formation can occur even when temperature limits are satisfied and global collapse is prevented. The analyses clearly showed that structural damage continues to evolve during the cooling phase, leading to additional cracking, hinge formation, and irreversible changes in internal force distribution. Neglecting the cooling phase may therefore result in a non-conservative assessment of post-fire damage. The case study further illustrated that substantial structural damage may develop even in tunnels equipped with passive fire protection. However, the results also

demonstrated that targeted protection of structurally critical regions, particularly the roof slab, can significantly reduce post-fire damage. Extending protection to less critical regions provided only marginal additional benefit, highlighting the potential for rational optimisation of passive fire protection strategies.

The proposed methodology translates detailed thermo-mechanical simulation output into interpretable damage states linked to indicative repair measures. At the same time, the study confirms that currently available damage classifications, largely developed for buildings, require further calibration for tunnel applications. In particular, the interpretation of plastic hinge formation, residual deformations, and large cross-sectional dimensions in terms of repairability remains an open research topic.

Overall, this study demonstrates the feasibility and added value of integrating nonlinear structural fire analysis with explicit post-fire damage quantification. The approach supports a transition from prescriptive temperature-based verification towards a performance-based evaluation of residual capacity and repairability, providing tunnel owners and asset managers with a more informed basis for decision-making after a severe fire events.

ACKNOWLEDGMENTS

Thomas Thienpont acknowledges the financial support of VLAIO on the research project ‘smartSFE’, Grant Number HBC.2024.0260. Balša Jovanović (Postdoctoral Fellow, 1264426N) is funded by the Research Foundation - Flanders (FWO).

REFERENCES

1. NFPA. NFPA 502 Standard for Road Tunnels, Bridges, and Other Limited Access Highways (2023).
2. Rijksoverheid. Bouwbesluit 2012 (Building Decree 2012). (2012)
3. ASTM International. ASTM E3134-17. Standard Specification for Transportation Tunnel Structural Components and Passive Fire Protection Systems (2020).
4. PIARC. Design criteria for structure resistance to fire. In: Systems and equipment for fire and smoke control in road tunnels. Technical report 2007 05.16.BEN (2007).
5. Franssen, J. M., Gernay; T. Modeling structures in fire with SAFIR®: theoretical background and capabilities. Journal of Structural Fire Engineering, 8 (3); 300–323 (2017). https://doi.org/10.1108/JSFE-07-2016-0010.
6. Ni, S., Gernay,T. A framework for probabilistic fire loss estimation in concrete building structures. Structural Safety, 88, 102029. (2021). https://doi.org/10.1016/j.strusafe.2020.102029.
7. CEN: EN 1992-1-2. Eurocode 2 - design of concrete structures. Part 1-2: general rules - structural fire design. (2004)
8. CEN: EN 1993-1-2. Eurocode 2 - design of steel structures. Part 1-2: general rules - structural fire design. (2005)
9. Annerel, E. Assessment of the Residual Strength of Concrete Structuresafter Fire Exposure. PhD thesis, Ghent University, Gent, Belgium (2010).
10. Chang, Y. F., Chen, Y. H., Sheu, M. S., Yao;, G. C. Residual stress–strain relationship for concrete after exposure to high temperatures. Cement and Concrete Research, 36 (10), 1999–2005, (2006). https://doi.org/10.1016/j.cemconres.2006.05.029.
11. Schneider, U., Nagele, E. Repairability of fire damaged structures. CIB, CIB W 14 report (1989)
12. Ingason, H., Gustavsson, S., Dahlberg, M.: Heat release rate measurements in tunnel fires. Swedish National Testing and Research Institute (1994).
13. Lucherini, A., Jovanovic, B., Merci, B., Van Coile, R.: Numerical analysis on the characterisation of the fire decay phase of post-flashover compartments. In: Proceedings of the 12th Asia-Oceania Symposium on Fire Science and Technology (AOSFST 2021). The University of Queensland, Online (2021).